Atmospheric Research 198 (2017) 22–33

Contents lists available at ScienceDirect

Atmospheric Research

journal homepage: www.elsevier.com/locate/atmosres

Weather forecast performances for complex orographic areas: Impact of different grid resolutions and of geographic data on heavy rainfall event simulations in Sicily

M.T. Caccamo[a], G. Castorina[a], F. Colombo[a,c], V. Insinga[b], E. Maiorana[b], S. Magazù[a,*]

[a] Department of Mathematical and Informatics Sciences, Physical Sciences and Earth Sciences (MIFT), University of Messina, Viale F. S. D'Alcontres 31, 98166 Messina, Italy
[b] Consorzio Interuniversitario Scienze Fisiche Applicate (CISFA), Viale F. S. D'Alcontres 31, 98166 Messina, Italy
[c] Italian Air Force Meteorological Service – Comando Aeroporto – Sigonella, Italy

ARTICLE INFO

Keywords:
WRF model
CORINE
ASTER
Heavy rain
Complex orography
Sicily

ABSTRACT

Over the past decades, Sicily has undergone an increasing sequence of extreme weather events that have produced, besides huge damages to both environment and territory, the death of hundreds of people together with the evacuation of thousands of residents, which have permanently lost their properties.

In this framework, with this paper we have investigated the impact of different grid spacing and geographic data on the performance of forecasts over complex orographic areas. In order to test the validity of this approach we have analyzed and discussed, as case study, the heavy rainfall occurred in Sicily during the night of October 10, 2015. In just 9 h, a Mediterranean depression, centered on the Tunisian coastline, produced a violent mesoscale storm localized on the Peloritani Mountains with a maximum rain accumulation of about 200 mm. The results of these simulations were obtained using the Weather Research and Forecasting (WRF-ARW) Model, version 3.7.1, at different grid spacing values and the Two Way Nesting procedure with a sub-domain centered on the area of interest. The results highlighted that providing correct and timely forecasts of extreme weather events is a challenge that could have been efficiently and effectively countered using proper employment of high spatial resolution models.

1. Introduction and synopsis

Extreme weather events are characteristics of the Mediterranean coastal areas and often cause flash floods. During these episodes, the precipitations that occur in a few hours often exceed the rain accumulations that normally occur in several months (Altinbilek et al., 1997).

Usually, these extreme precipitations are in conjunction with intense and quasi-stationary mesoscale convective phenomena that insist on the same area for several hours (Fiori et al., 2014). Local factors such as the presence of orographic reliefs along to the coastline often determine their intensity. The geographical position and the complex orography of Sicily often cause extreme weather events (Chen and Lin, 2005; Chen and Sun, 2002). Positioned at the center of the Mediterranean Sea, the island is placed in the transition zone between the arid and dry climate of North Africa; the more temperate and humid climate of central Europe. Hence, the phenomena trigger the interactions between processes typical of middle latitudes and the tropics.

In early autumn, the Mediterranean cyclones that originate from the contrast between air masses with very different temperatures and humidity interacting with seawater high temperature (Sea Surface Temperature, SST), affect the seas surrounding Sicily. These conditions can cause extreme weather events characterized by sudden and heavy rainfalls and dangerous flash floods (Cassola et al., 2015).

From the geographic point of view, Sicily is characterized by an orography distributed in the direction of the parallel, especially in the Northern area, which is strongly exposed to the atmospheric perturbations that come from the South. In such cases, the warm and moist air coming from the Libyan Sea is often lifted over the orographic barriers, losing its humidity because of the cooling, and these modifications can cause heavy rains (Chu and Lin, 2000; Randall, 2001). This occurs especially in the autumn seasons when the sea around the island is still warm and able to transfer large amounts of humidity into the atmosphere (Giuffrida and Sansosti, 2007; Salby, 1996).

It clearly emerges that the island complex orography plays a key role in the portion of the Ionian coastline between the towns of Catania and Messina (Fig. 1).

In detail, our work covers an area where the most important

* Corresponding author.

http://dx.doi.org/10.1016/j.atmosres.2017.07.028
Received 18 October 2016; Received in revised form 12 June 2017; Accepted 30 July 2017
Available online 07 August 2017

Fig. 1. 3D Orography of the eastern coast of Sicily between Catania and Messina.

morphological structures are the massif of Mt. Etna (3330 m above sea level) and the Peloritani mountain range (max altitude is 1374 m ASL), which stretches between the Mt. Etna and the Strait of Messina for a length of approximately 65 km.

Between these mountains is the Alcantara Valley, located North of Mt. Etna, and some other smaller valleys that descend from the Peloritani Mountains following the NW-SE direction towards the sea.

Recently, extreme weather conditions have affected this area of Sicily. For example, from the tragic sequence of severe meteorological events that occurred between 2007 and 2011 in the below towns:

i) 25 October 2007, which took place at Santa Margherita, Giampilieri and Scaletta (Messina), with flash flood and precipitations of 175 mm in 2 h, against an annual average amount of 800–1000 mm;
ii) 22 November 2011 at Barcellona and Saponara (Messina) with precipitations of 351 mm in 10 h (recorded by the Castroreale weather station);
iii) 01 October 2009 at Giampilieri, a tragic and disastrous event with 37 victims.

Referencing these three events, the recovery costs of the disaster damages were estimated at about 900 million euros (Source: DRPC Sicily – Stato dei rischi del territorio Siciliano – Rischio idrogeologico: raccolta dati storici – Sicilian Territory State of Risk – Hydrogeological Risk: Historical data Record). These events, occurred during the beginning of the autumn season, did not originate from a single factor, but rather from a sum of several interacting processes at different scales not yet fully understood. Consequently, their study can represent a big chance for testing the performances of High Resolution Meteorological Models, which as of yet have not been able to effectively predict the amounts of precipitation with the required spatial and temporal accuracy (Davolio et al., 2009; Miglietta and Rotunno, 2009). Topography and land use characteristics at the respective scales strongly influences the local and regional weather and climate (Clyne and Rast, 2005; Garratt, 1993).

While the climate modeling community is performing runs typically at grid spacing of 100 km, 50 km or at most, 10 km, higher resolutions are needed for places with complex topography (Szintai et al., 2010; Schicker and Seibert, 2009; Zängl, 2007) and dynamical downscaling seems to be the way to go. The Meteorological Models local circulations accurate simulation ability will rely strongly on resolving the important terrain features over focused area. Since the terrain height depends on the grid resolution model, it is essential that the simulation uses an adequate grid size in order to resolve the terrain forcing over the analyzed area (De Meiji and Vinuesa, 2006; Clyne et al., 2007; Kalnay, 2002; Haltiner & Williams, n.d.). Merging high-resolution topography, up-to-date land uses, vegetation fraction and soil moisture and temperature are fundamental to allow models perform realistically at high resolutions, with correct atmosphere-surface interaction (Arnold et al., 2012). The aim of this paper is to understand which effects will produce an improved topographic representation obtained using different grid interval and a use of different geographic data, on the rainfall field forecast.

2. Description of the case study

The selected case study concerns a recent flood event that occurred in Messina in the early hours of 10 October 2015. In the case study, the Antillo meteorological station, which is a unit of DRPC (Dipartimento Regionale della Protezione Civile – Regional Civil Protection Department) weather stations network, recorded, from 00 to 09 UTC, a maximum precipitation accumulation of 175,4 mm. The heavy rains occurred, were the results of a mesoscale convective system developed in the Ionian Sea and powered the low atmospheric layers by the very humid Southeastern streams (Ray, 1986; Wallace and Hobbs, 2006). Another important element that triggered the violent thunderstorm was the orographic lift induced by the barrier of Nebrodi and Peloritani Mountains, together with the one induced by Mt. Etna.

The surface analysis chart at 00:00 UTC of 10 October 2015, shows a low-pressure system centered over the Central Mediterranean Sea, originating a Mediterranean cyclone, with its warm branch extended between the Southern coast of Sardinia and the Greek coast, while the cold branch was affecting the North to South, all over Tunisia. The

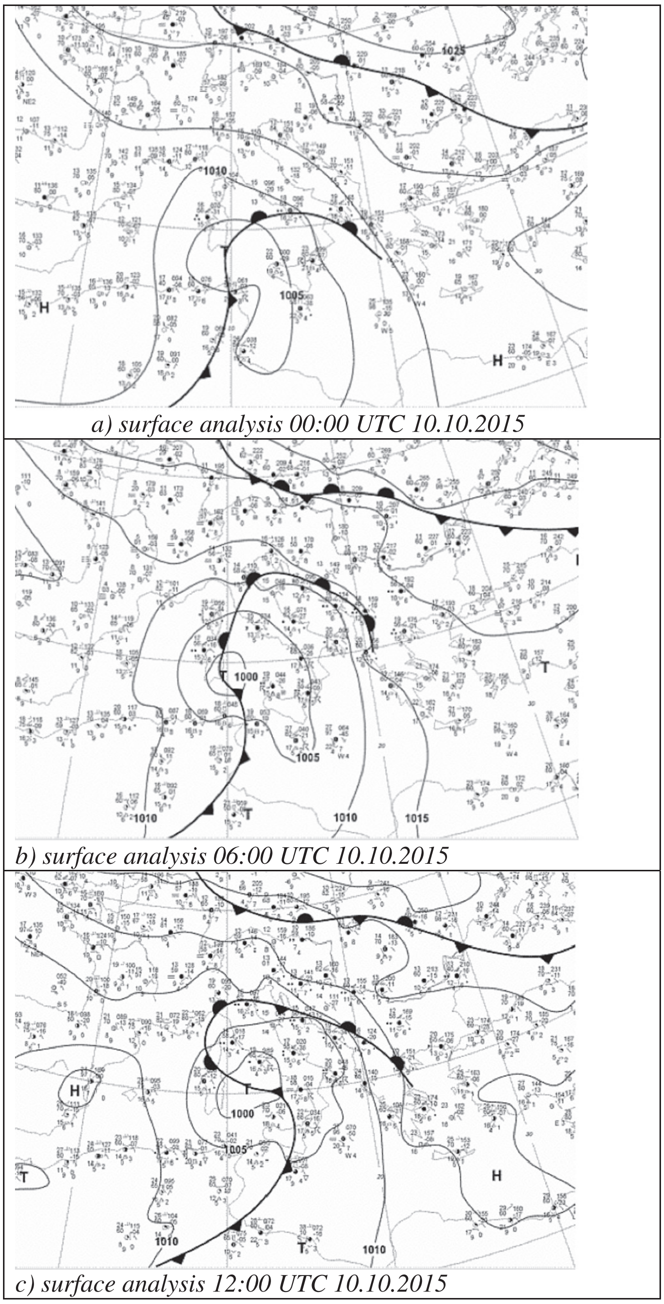

Fig. 2. Time shots of surface maps (a, b and c) at 00:00, 06:00 and 12:00 UTC on 10 October 2015.

winds on the Eastern Sicily reinforced maintaining a S-S-E component. The air temperatures were a few degrees lower than the sea surface one. The weather station of Messina reported thunderstorms (Fig. 2a).

At 06:00 UTC of 10 October 2015, the low-pressure over Southern Sardinia deepened reaching values below 1000 hPa. The cold air approached the Western coast of Sicily reduced the temperature by 6–8°. The winds along the eastern coast of Sicily maintained a southern component, while all the Sicilian weather stations have registered thunderstorms (Fig. 2b).

At 12:00 UTC of 10 October 2015, the low pressure moved to the central Tyrrhenian sea, maintaining pressure values below 1000 hPa. The cold front crosses all of Sicily, also affecting the Central Tyrrhenian Sea and Malta (Fig. 2c).

The synoptic analysis allowed us to formulate the following

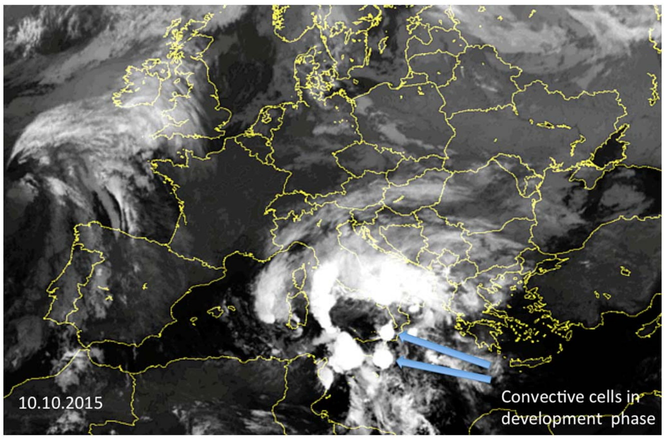

Fig. 3. Thermal infrared MSG image at 03.00 UTC of 10 October 2015.

hypotheses about the causes that led to the event:

1. The intense S-E flux, affected the Ionian coast throughout the whole event interval and it funneled huge volumes of warm air from Libya to the central Tyrrhenian Sea. In addition to the heat content, this air mass was self-enriched with water vapor, largely drawn from the Gulf of Sirte, where SST ranged between 25 °C and 26 °C, as registered by the Italian Air Force Weather Service. These circumstances allowed the air masses with high values of equivalent potential temperature to rise in the lower atmosphere layers. Then, the potential energy available for convection (CAPE), reached peak values higher than 4000 J/kg on the Southern seas of Sicily (GFS model analysis data). Under such circumstances, both the Alcantara Valley and the side valleys of the Peloritani chain played a key role in conveying high volumes of warm and moist air to advance for several tens of kilometers inland;
2. The forced lifting due to the Peloritani Chain, which turns almost perpendicularly to the ground flow, facilitated the warm and moist air mass initial lift, and the same occurred to the SE air streams due to Mt. Etna;
3. The arrival of a little pulse of cool air, probably connected to the action of a convective cell in Western Sicily made it possible for the development of the entire cluster of storms, according to the well known "multicell cluster storm" scheme.

The outcome of the above-mentioned factors was the development of two convective cells, visible in the 03.00 UTC infrared image (Fig. 3), which affected the entire Ionian coast of Sicily with heavy rainfalls and severe thunderstorms (Morrison and Milbrandt, 2011).

In other words, it can be inferred that the trigger of this event was an initial lift of a layer of warm air next to the surface, supported in its upward movement by the high altitude flow perturbation produced by Mt. Etna, due to strong upper-air southwesterly wind streams.

Despite the short duration, these phenomenas were powerful enough to produce a greater accumulation of rain of 175 mm, as recorded by Antillo weather station (Fig. 4). This quantity of rain was sufficient to determine the Mela creek overflow and the flash flood that occurred in Milazzo and Barcellona Pozzo di Gotto, both located on the Tyrrhenian coastline.

3. Impact of horizontal resolution for the forecasting of mesoscale thunderstorm events

A mountain barrier determines a considerable effect on atmospheric circulation and may significantly influence the weather forecast. In fact, the discontinuities of the earth's surface, i.e. a complex orography, may

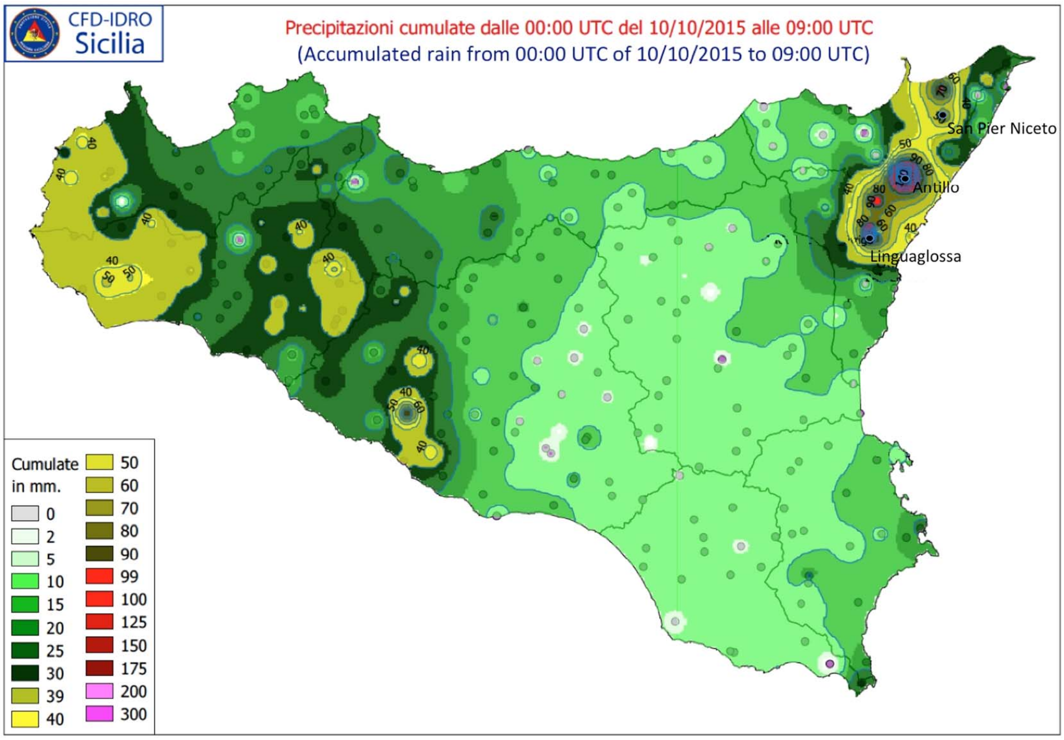

Fig. 4. Precipitation observed by the monitoring network of the Regional Department of Civil Protection.

affect the motion of atmospheric circulation at all scales, determining sometimes a strong change in wind direction and intensity (Reeves and Rotunno, 2008). Therefore a detailed analysis of both boundary conditions and orography is often a crucial element in the development of an effective meteorological model (Smith, 1979).

In the presence of orographic forcing, such as those generated by very high reliefs - in our case Mt. Etna and Peloritani Mountains – an increased spatial resolution may allow to explore relevant scales of air motions which otherwise should not have been taken into account in the simulation.

This work presents a comparison of the findings obtained by numerical simulations performed at different spatial resolutions together with the employment of different approaches for the model initialization process (Buzzi et al., 1998).

More specifically, in this study we compare the simulation results obtained by using an initial configuration run characterized by a horizontal grid spacing of 10 km and those obtained by using a Nesting Two Way configuration with a subdomain horizontal grid spacing of 0.8 km and a parent domain with a horizontal grid spacing of 4 km.

This study mentions all configurations developed using the WRF-

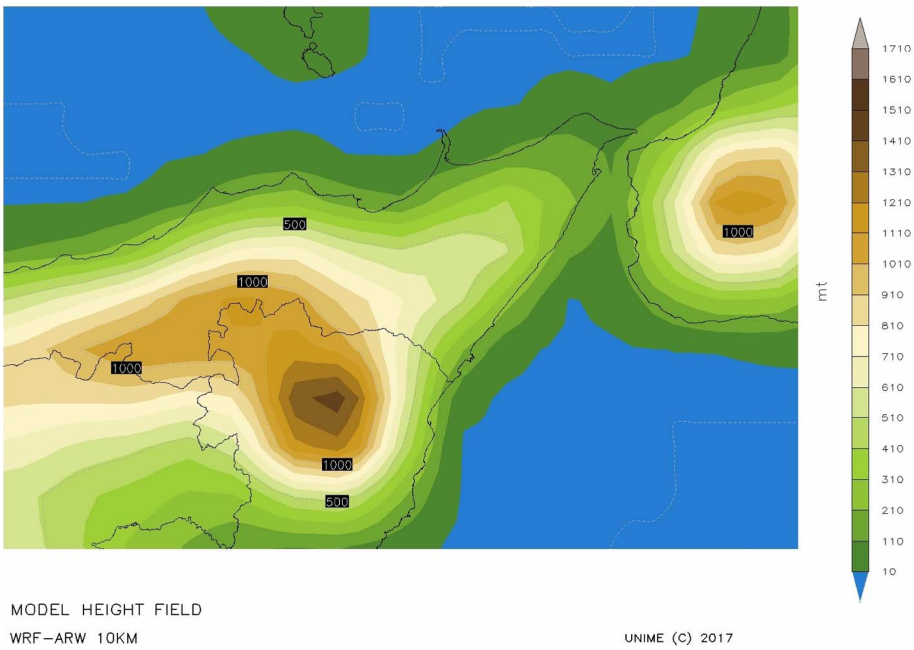

Fig. 5. Topography obtained by WRF with spatial resolution of 10 km. Heights are in meters.

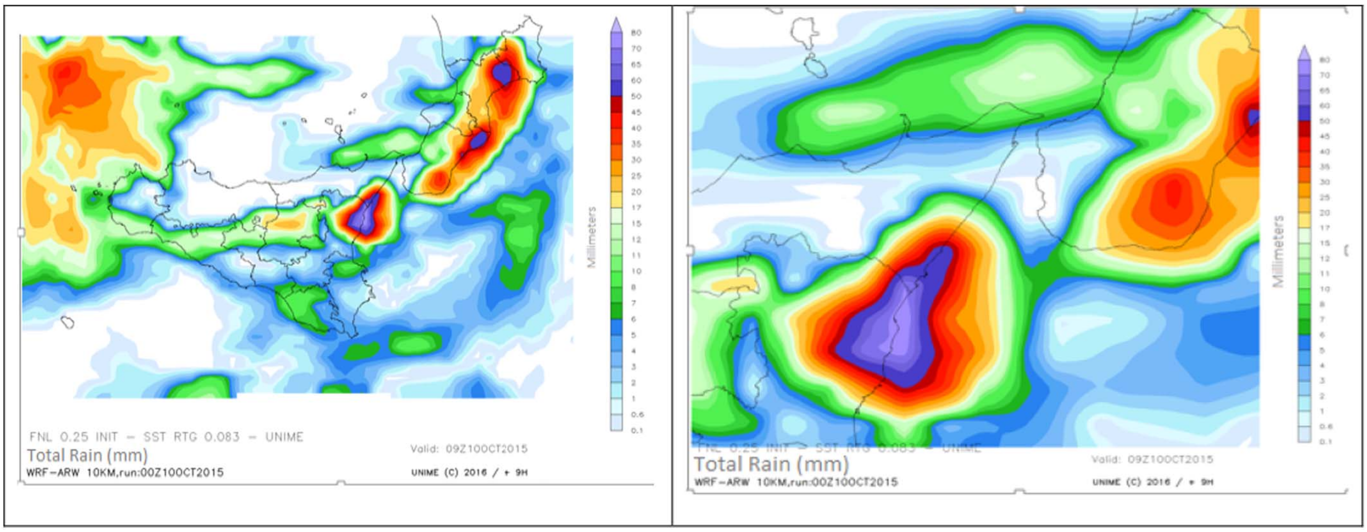

Fig. 6. Accumulated precipitations forecast by WRF with resolution at 10 km(left) and zoomed detail over North-Eastern Sicily (right) from 00 to 09 UTC.

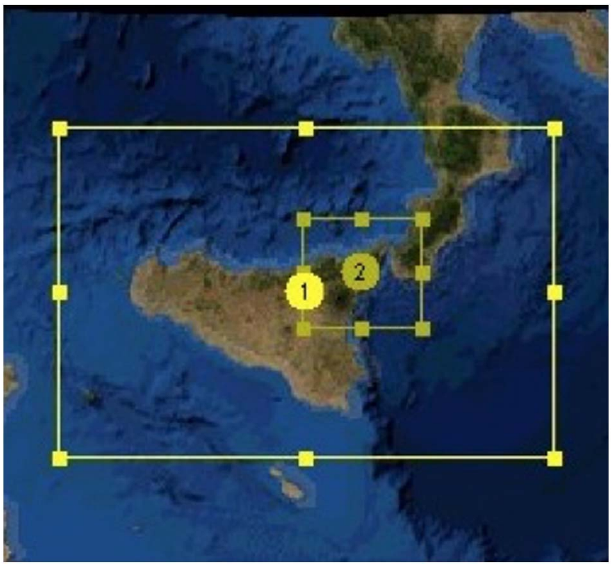

Fig. 7. Nesting Two Way: parent domain with horizontal grid spacing of 4 km and subdomain with horizontal grid spacing of 800 m.

ARW, version 3.7.1, together with non-standard geographic data. The GTOPO30 digital elevation model developed by USGS working at 30 arcsec resolution has been replaced by the ASTER GDEM V2 model, as a result of the collaboration established in 2011 between METI (Ministry of Economy, Trade, and Industry of Japan) and NASA, characterized by a 1 arcsec resolution.

The USGS data (Landuse) at a 30 arcsec resolution were replaced by Corine Land Cover 2006 data, developed by EEA (European Environment Agency) characterized by a 3 arcsec resolution, reclassified on 24 classes of Landuse (Pineda et al., 2004).

The global model NCEP FNL at 0.25° with a time interval resolution of 3 h, processed for the 00Z run relative to the 10 October 2015 have generated the initial and boundary conditions. Were used the RTG sea surface temperature data with a resolution of 0.083°. For long-wave radiations the RRTM (Rapid Radiation Transfer Model) scheme was used (Mlawer et al., 1997), while for the short-wave radiations the Goddard scheme (Chou and Suarez, 1994). In addition the above, were also used the schemes of Mellor-Yamada-Janjic (Janjic, 2002) for the boundary layer and Noah land surface model (Chen and Dudhia, 2001).

The microphysical scheme utilized was the Thompson (Thompson et al., 2004) a well known double-moment scheme widely tested especially in high-resolution simulations. In the Nesting Two Way simulations for the parent-domains, the Kain Fritsch convective scheme (Kain, 2004) was used, while for the subdomains the resolution of convective processes was explicit.

A number of 65 vertical levels with higher resolution for the levels close to the surface and to the top of the air column using a vertical distribution with hyperbolic tangent were employed using the WRF software DOMAIN WIZARD distributed by NOAA.

The determination of the configuration with horizontal grid spacing of 10 km came out by a single-run that covered a wide area with extension from latitude 30.03° to 44.35° and longitude from 2.67° to 25.64°.

For a LAM with a horizontal grid spacing of 10 km, the actual topography cannot be clearly represented because of the grid sizes (see Fig. 5)

With this grid spacing, the complex orography of S-E Sicily representation that includes Mount Etna, Nebrodi and Peloritani looks alike as a single mountainous relief, with heights far lower than the real ones (Davolio et al., 2006; Hoskins and James, 2014). The error that this topographic modeling generates, among others, affects two aspects of considerable importance for the formulation of weather forecasts: the estimation of vertical speeds and the flow divergence, and the latter affect, in a considerable way, the genesis and the development of heavy rainfalls with the results of a non-realistic simulation (Fig. 6).

4. Nesting configuration

Regarding nesting configurations, there are two possible options to select at the launch of each simulation:

- One-Way Nesting where the exchange of information between the father domain (parent domain) and the subdomain is unidirectional, since the subdomain uses the boundary conditions of the already processed parent domain, without performing a feedback procedure of the parent domain, which is coarser. The sub-domain receives the Lateral Boundary Conditions (LBC)(parent domain) on a 3-h basis.
- Two-Way Nesting where the exchange of information between the parent domain and the subdomain is bidirectional. In such cases the feedback procedure influences the performance of the parent domain. The LBC of the subdomain includes microphysical variables and vertical movement and the subdomain uses the LBC of the

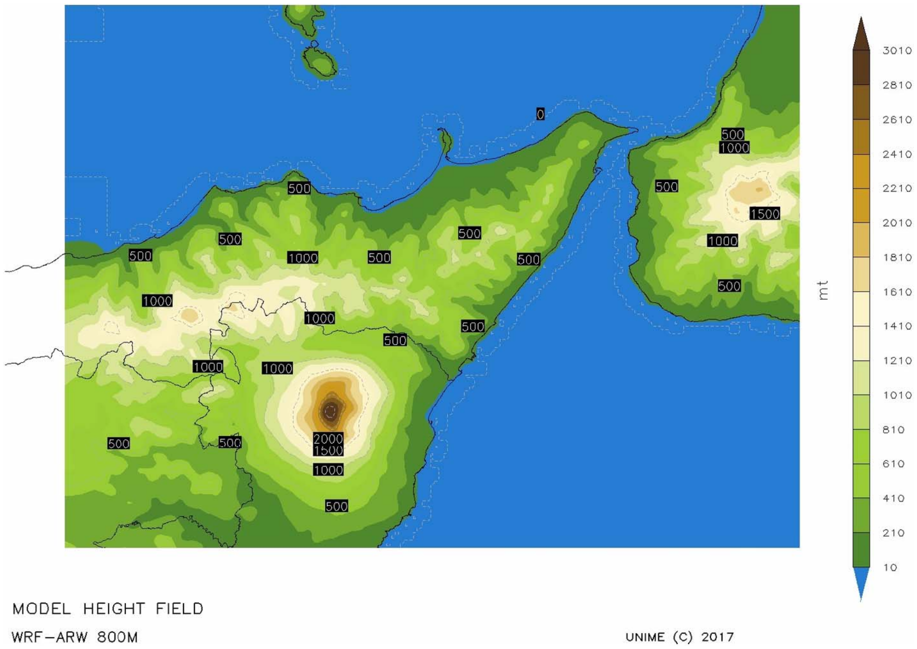

Fig. 8. Orography of WRF at 800 m of horizontal grid spacing.

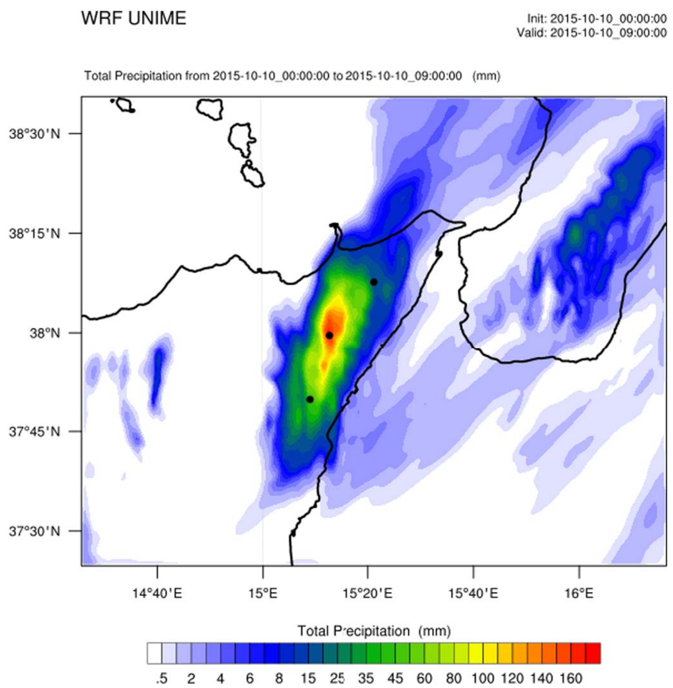

Fig. 9. Precipitation provided by WRF in NESTING TWO WAY configuration with a horizontal grid spacing of 800 m. The black dots show the position of the weather stations of San Pier Niceto, Antillo and Linguaglossa (from North to South).

parent domain at each time step (T + nestT).

The relevant factor to obtain good precipitation prediction has been attributed to the utilization of the Two-Way Nesting technique instead of a single-run configuration. While single-run uses Global Model data as boundary conditions, with lower resolution and, in the case of FNL, three-hours of input frequency, in the Nesting approach, the subdomain with a higher resolution uses as LBC the father domain (parent domain), which has a better vertical and horizontal resolution than the Global Models conditions. In addition, the parent domain provides the sub-domain LBC at each timestep (T + nestT).

T = Timestep (Parent Domain)/nestT = Timestep subdomain (T/ratio)

In order to develop and refine the forecast's effectiveness, we increased the horizontal spatial resolution for a more correct treatment of the altimetry, improving the mountain systems localization (Holton, 2004; Markowski and Richardson, 2010; Martin, 2006). The setup used for the analysis of the event is defined by Two Way Nesting with a horizontal grid spacing of 4 km (parent domain) extended to the entire area of Sicily, surrounding seas, and a sub-domain with a horizontal grid spacing of 800 m. (ratio 1:5), limited to an area including Mt. Etna, Messina and the Calabrian coastline (Fig. 7).

As we shall see, although the adopted procedure required remarkable computational resources, the obtained results fully justify such procedure. The new simulation obtained at this grid spacing, shows the SE flow in the lower layers, to impact against the massive mountain system constituted by the Eastern side of Mt. Etna triggering a remarkable Stau effect by adiabatic expansion of the mass air rising the mountain slope. On another note, with 800 m of grid spacing, the altitude of Mt. Etna reaches 3010 m ASL, vice 1500 m ASL with 10 km of grid spacing. The Peloritani mountains, poorly represented in the version with 10 km of grid spacing, now constitute a mountain set very close to the sea of about 1000 m. height (Fig. 8). In the Two Way Nesting simulation with a sub-domain at 800 m. of grid spacing, the phenomena result strongly enhanced by orography, revealing a great foresight performance of the V-Shape thunderstorm that affected Messina on the night of 10 October 2015 (not shown).

As mentioned above, the improvement of the rainfall forecast (Fig. 9), in this case is due to a higher resolution of the orography, i.e. by a better representation of Mt. Etna, Peloritani and Nebrodi mountains and combined wind field effects (Fig. 10).

As we shall see, during the whole process, the differences in the wind fields at 10 m played a key role. With the 10 km model, there is a small area of convergence only; Mt. Etna induces it in the lower layers, generating a rainy core on the Ionian Sea. With the 800 m model, 10 m height winds with a mean velocity of about 90 km/h generate a strong Stau effect on the Eastern side of the Peloritani Mountains, while the Tyrrhenian side received only a few mm of accumulation (rain shadow

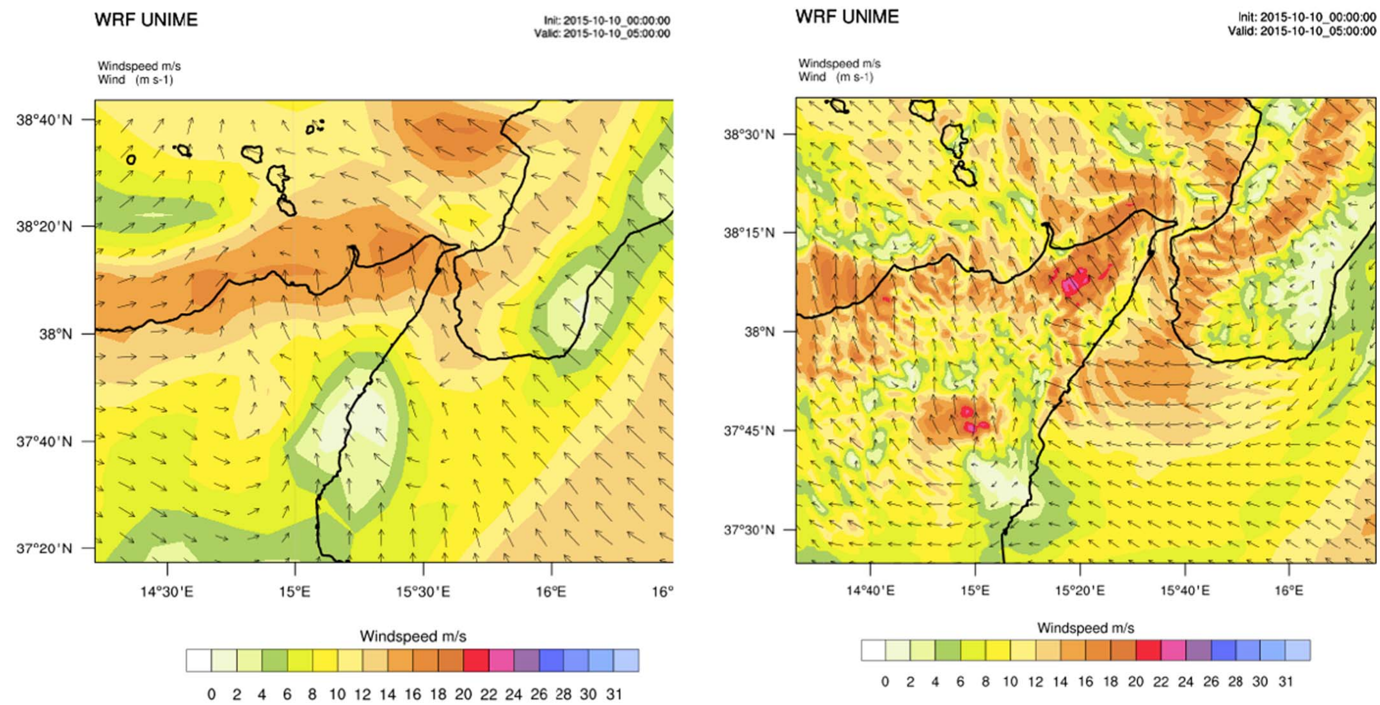

Fig. 10. 10 m. wind field forecast at 05:00 UTC by the WRF 10 km (left) and 0.8 km (right).

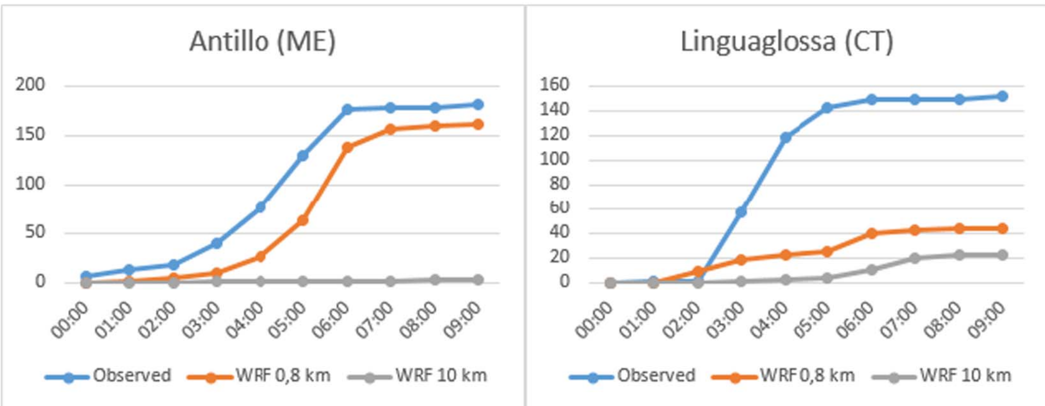

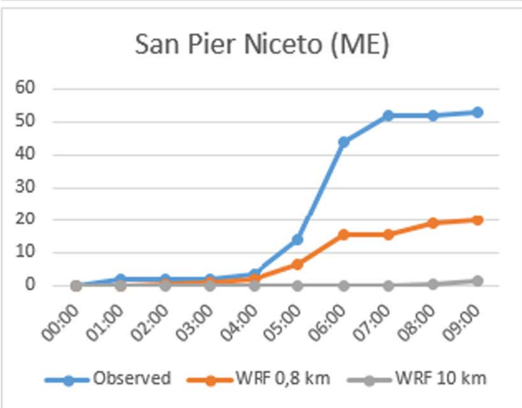

	Antillo	Linguaglossa	San Pier Niceto
Observed	*182 mm*	*152 mm*	*52,8 mm*
WRF 0,8 km	*161,1 mm*	*43,9 mm*	*19,7 mm*
WRF 10 km	*2,6 mm*	*21,8 mm*	*1,3 mm*

Fig. 11. Antillo, Linguaglossa and San Pier Niceto weather stations: observed rain (blue), WRF 0,8 km forecast (red) and WRF 10 km forecast (grey) versus time. Bottom right: Total accumulated precipitations observed and forecast. (For interpretation of the references to color in this figure legend, the reader is referred to the web version of this article.)

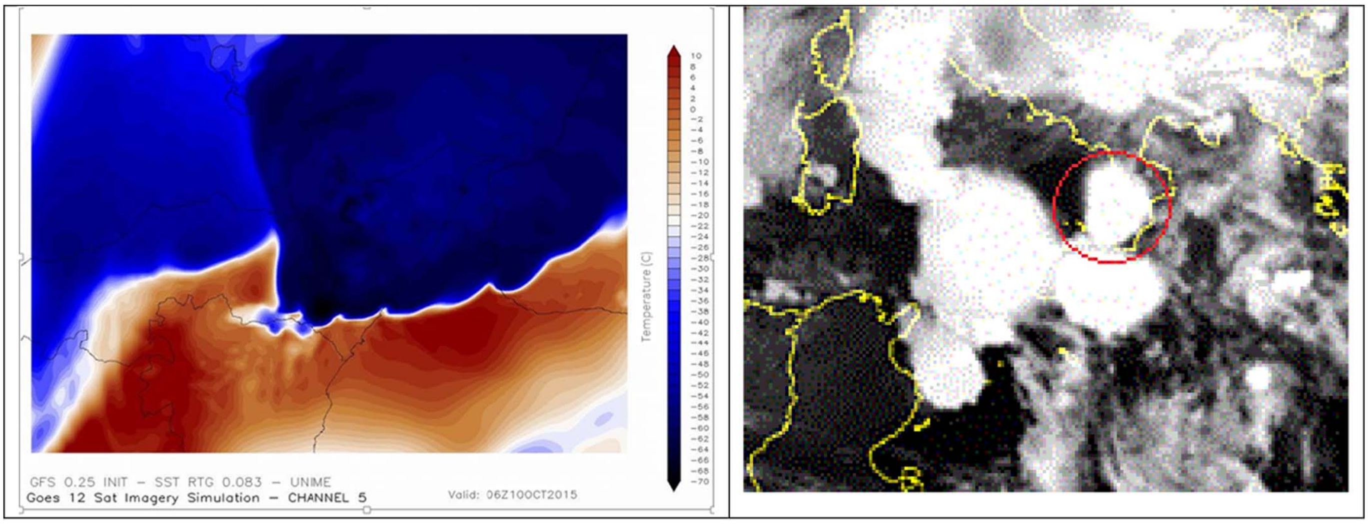

Fig. 12. Comparison of WRF simulation and satellite observation Sat MSG at 06:00 UTC.

Table 1
Composition of standard and HD geographic data.

	DEM	LAND-USE
Standard data	GTOPO 30	USGS30
HD data	ASTER	CORINE

effect). It is also evident the "turbulent friction" caused by Mt. Etna, producing a deviation to east of the low-level jet and the genesis of an area of convergence. The tests performed on the 10th of October 2015 episode shows that the WRF model configured via Two Way Nesting with subdomain centered in the area affected by the heavy precipitation provides good results in Peloritani area. In particular, they regard the position as well as the amount of the occurred precipitations. The verification has been extended to 3 weather stations: Antillo, Linguaglossa and San Pier Niceto. The position of each weather station is visible in Fig. 1, Fig. 4 and Fig. 9. The model performance is excellent at Antillo (rainfall peak). The total precipitation amount is significantly underestimated in Linguaglossa and San Pier Niceto, but the 4 km–0.8 km configurations improve the simulated precipitation relative to the 10 km grid.

The forecast data from WRF output are visible in Fig. 11, compared with observed data.

The comparison between the GOES 12 Sat Imagery Simulation generated by UPP software and the MSG satellite picture is very impressive (Fig. 12).

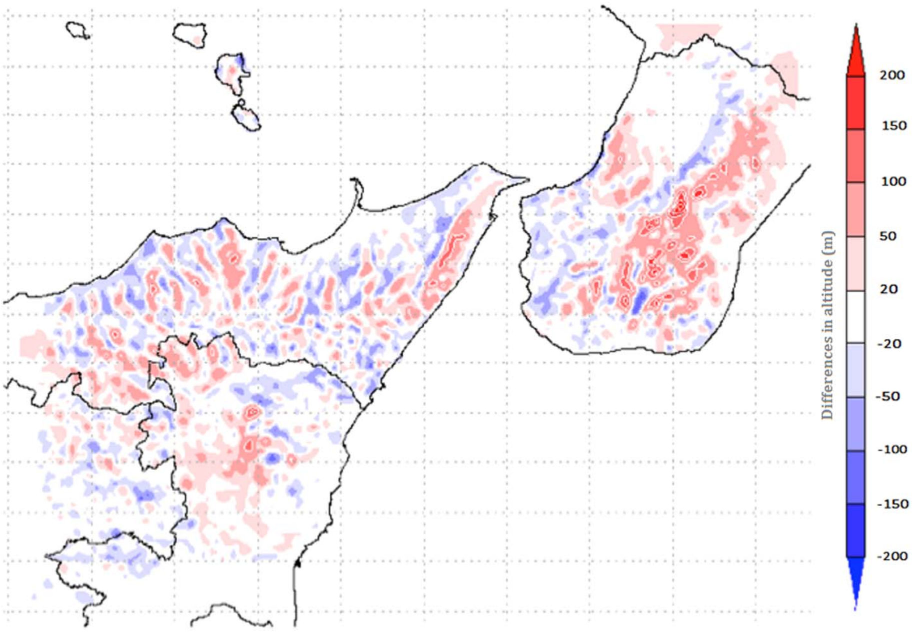

Fig. 13. Differences in altitude between ASTER V2 DEM (res: 30 m) and GTOPO30 (res: 1 km) on a 800 m domain.

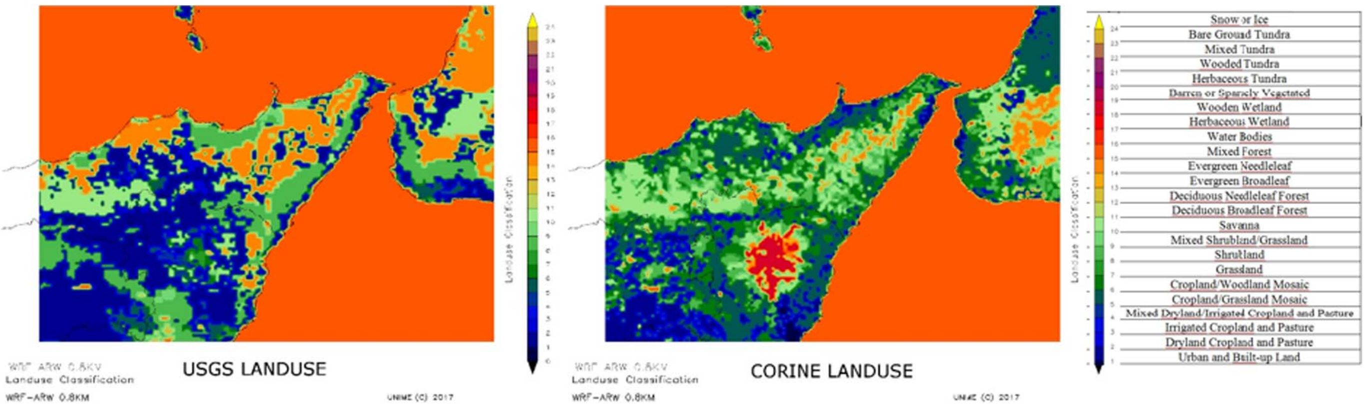

Fig. 14. USGS land-use and CORINE land-use on model domain.

5. Impact of alternative geographic data for the mesoscale forecasting of rain events

As we described in the introduction, in this case study, the definition of different geographic data utilization impact study is reached by performing a new run through the Two Way Nesting approach. The parameterizations used are identical to that described in the previous paragraph, with the replacement of alternative geographic data with those distributed along with the standard model WRF (Table 1).

The following image describes the orographic differences attributable to the use of ASTER GDEM V2 data rather than GTOPO30 data (Fig. 13) (Stensrud, 2007; Miglietta and Buzzi, 2001; Haltiner and Williams, 1983a; Lackman, 2011).

Although both forecasts do not show many differences, with regard to the spatial location of the event, a better representation of the terrain obtained with the utilization of finer DEM and Land-se data (Fig. 14), had a positive impact on the precipitation amount forecast. Different types of Land use have different physical properties that can change the radiation and energy balances and hence vertical fluxes of moisture, heat and momentum, which also lead to changes in temperature, and moisture fields near the surface (Esteve, 2014). For example in presence of vegetative cover we have to consider the "evapo-transpiration" process. The surface energy and moisture budgets for bare and vegetated soils are crucial during typical thunderstorm weather conditions. Changes in land-surface properties are shown to influence the heat and moisture fluxes within the planetary boundary layer, convective available potential energy and other measures of the deep cumulus cloud activity.

Hence, the change of Land-use data has a strong impact on the precipitation field, especially in presence of complex orography and with grid spacing smaller than 1 km.

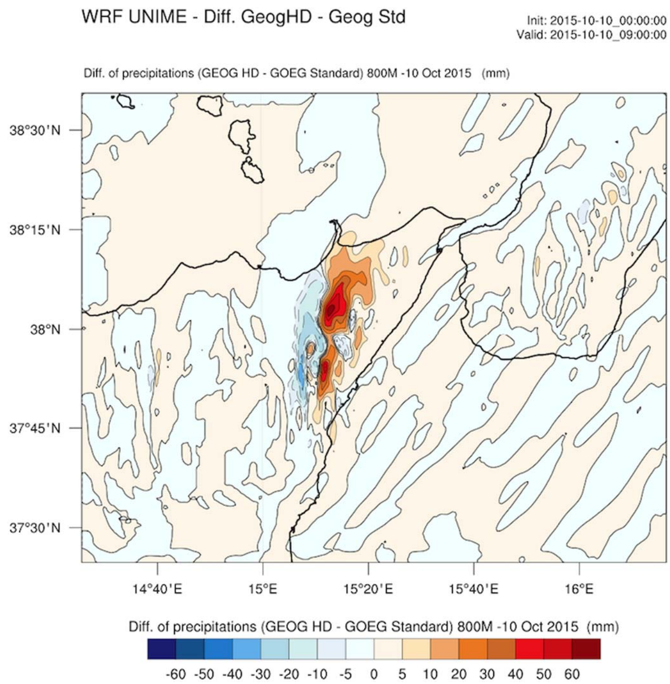

Fig. 15. Run 800 m - final accumulations differences (GEOG STANDARD - GEOG HD).

In Table 2 and in detail, in Fig. 15, it is possible to highlight how the resulting differences obtained reaches in some areas also 60 mm.

The increase of the spatial resolution from 10 km to 4 km and then to 800 m, besides to substantially improve the territory representation,

Table 2
Accumulated precipitation observed in Antillo, Linguaglossa and San Pier Niceto and forecast by WRF with 800 m of grid spacing using Standard and HD geographic data.

	Antillo OBS	800 m HD	800 m SD	Linguaglossa OBS	800 m HD	800 m SD	San Pier Niceto OBS	800 m HD	800 m SD
10/10/15 00:00	0	0	0	0	0	0	0	0	0
10/10/15 01:00	0,6	1,3	0,4	0,6	0	0	1,8	0	0
10/10/15 02:00	6,2	3,9	3,6	0,8	8,3	9	1,8	0,5	0,5
10/10/15 03:00	29,6	9,1	8,8	56,8	18,3	17,7	2	0,7	0,8
10/10/15 04:00	68,1	26,1	32,7	118,6	22,2	21,5	3,2	1,8	2,3
10/10/15 05:00	121,7	62,4	63,7	142,8	25,2	28,9	13,6	6,4	3,6
10/10/15 06:00	169,9	139,3	86,2	149,4	39,8	34,3	43,8	15,3	12,9
10/10/15 07:00	171	157,2	113,4	149,6	42,2	36,4	51,8	15,6	13,1
10/10/15 08:00	171	160,2	116,1	149,6	43,9	39,5	52,2	18,7	15,4
10/10/15 09:00	175,4	161,2	117,2	151,8	43,9	39,5	53,2	19,8	15,9

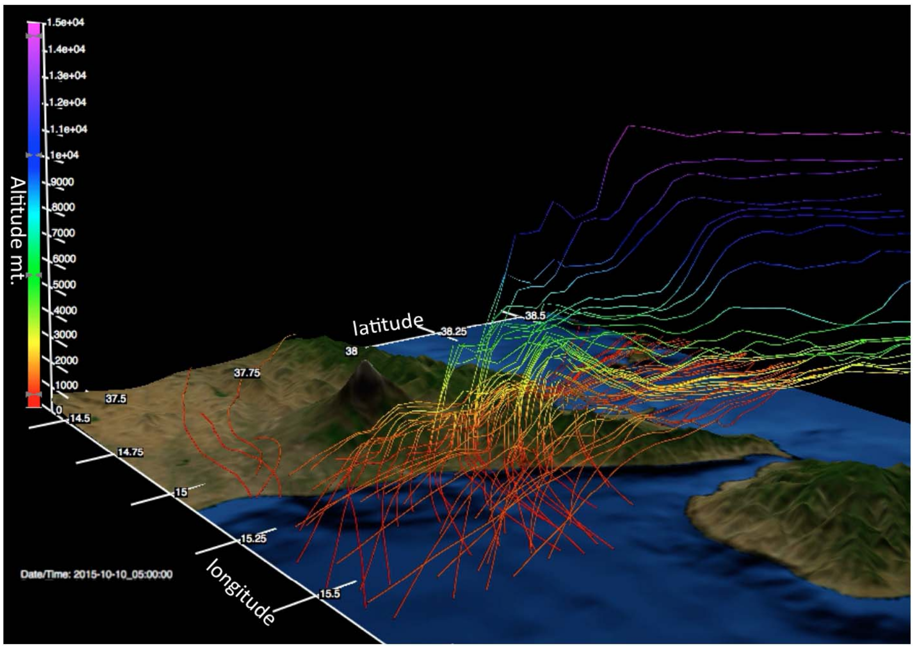

Fig. 16. 3D representation of the air flows of 10th October 2015, 05:00 UTC colored by altitude obtained by WRF 800 m on domain 2 of Fig. 7.

has allowed a larger detail for the main meteorological fields investigated, facilitating the understanding of the phenomenon itself. For example, looking at the synoptic analysis only, it is unclear if the air stream disturbance induced by Mt. Etna, has or has not played a decisive role. The image of the "stream" air flows (Fig. 16), rebuilt starting from the output of the model at 800 m resolution through the Visualization and Analysis Platform for Ocean, Atmosphere, and Solar Researchers (VAPOR) software, highlights and clarifies many relevant aspects:

- The Southeastern surface flow, as soon as it starts to rise, is immediately "caught" by the Southwestern one, predominant at 500 hPa level;
- The initial lift, finds a preferential path in Alcantara Valley allowing the warm and humid currents to climb the course of the valley for several tens of kilometers, before being raised;
- After an initial lift, a new pulse, stronger than the first one and generated by Mt. Etna, leads the air particles to rise up to quotes next to tropopause (Fig. 16).

A cross-section taken parallel to the coastline shows the vertical speed and the flows in the lower layers (Fig. 17) that lead the thunderstorm development. The model forecast of vertical wind component (w) shows extreme values till 24 m/s.

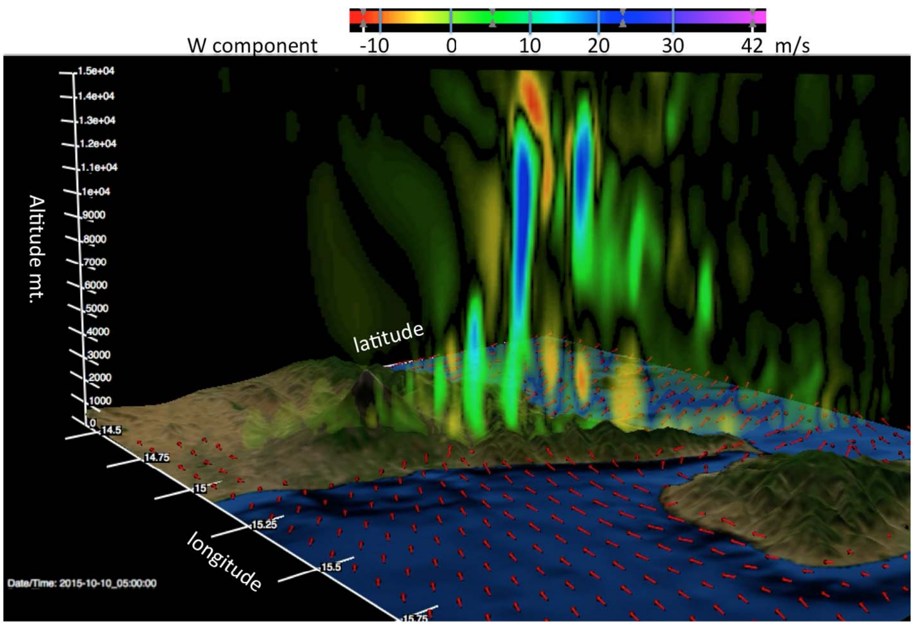

Fig. 17. Vertical component of the wind velocity (m/s) at 05:00 UTC on a coastline parallel cross-section on domain 2 of Fig. 7.

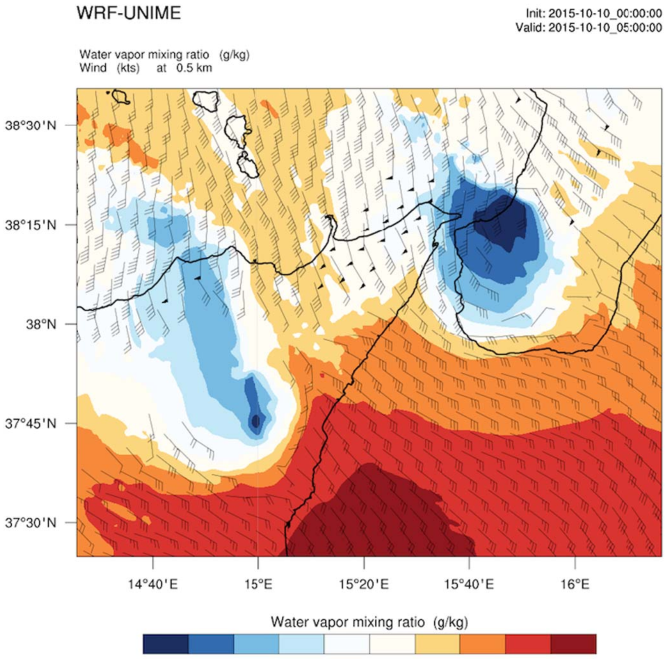

Fig. 18. Amount of vapor (g/kg) in the lower atmosphere (500 m ASL) and wind flows in kts at 05:00 UTC on domain 2 of Fig. 7.

Another aspect that the model with a 800 m of resolution allows to understand is the so called "Alcantara effect." Such "effect" is related to the role of the Alcantara Valley, which in the case of ground flows, coming from southeast would facilitate the entrance into the hinterland of huge volumes of moisture for several tens of kilometers. Air is forced to rise along the highest part of the Alcantara basin facilitating the condensation of water vapor and the subsequent development of convective clouds. This situation occurred in the early hours of October 10th and has been fully rebuilt by this simulation. The map in Fig. 18 shows the water vapor mixing ratio field in g/kg in the lower portion of the atmosphere (500 m ASL) as obtained by WRF 800 m. where is clearly visible the Alcantara effect.

The 800 m resolution has also allowed for the rebuilding of the thundercloud structure, visually noticeable in Fig. 19. The highlighted portion is not only the morphological structure of the thunderstorm cell, but also the top altitude reached by cumulonimbus. The image is obtained by plotting the cloud fraction (CLDFRA) field of WRF by VAPOR software using the Direct Volume Rendering option.

6. Conclusions

The purpose of the numerical simulations carried-out with the use of WRF-ARW model, properly set and configured for Sicily, was to find out the best compromise between the finest spatial resolution and the available calculation capacities to obtain the best timely forecast possible. To pursue these results, tests were conducted using different configurations. The stormy event of 10 October 2015 was used as a "case study" and has allowed us to compare the data collected from weather station networks available in Sicily with the model outputs. In particular, we have compared the amount and distribution of rainfall, using two WRF configurations. The first one employed a run with 10 km grid-spacing, while the other one used two two-way nested domains with 4 km and 0.8 km grid-spacing.

Similar tests were performed using ASTER GDEM V2 data rather than GTOPO30 data, as well as replacing the USGS Landuse data with Corine Land Cover 2006 data.

A direct comparison between the observed and forecast data has also been performed using Antillo, Linguaglossa and San Pier Niceto weather stations record and focus on the Nebrodi range.

The obtained results consented to clearly show that the improvement of the model grid spacing, together with the use of more accurate geographic data and the land use data, more suitable for the description of the territory, are the key elements for the prediction accuracy. This is especially true for geographic areas like Sicily that are characterized by the presence of complex orographic structures.

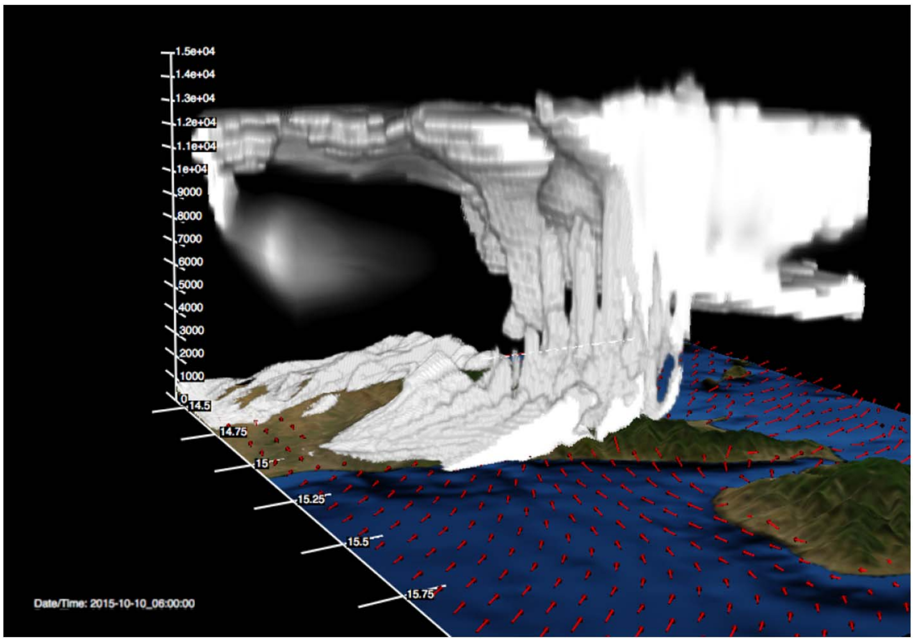

Fig. 19. Structure of the thunderstorm cell at 06:00 UTC obtained plotting a Direct Volume Rendering of CLDFRA field with isosurface = 1 and surface wind (red arrow) of WRF 800 m on domain 2 of Fig. 7. (For interpretation of the references to color in this figure legend, the reader is referred to the web version of this article.)

Acknowledgements

The authors wish to acknowledge the Dipartimento Regionale della Protezione Civile Regione Sicilia.

References

Altinbilek, D., Barret, E.C., Oweis, T., Salameh, E., Siccardi, F., 1997. Rainfall Climatology on the Mediterranean in EU-AVI 080 Project ACROSS — Analyzed Climatology Rainfall Obtained from Satellite and Surface Data in the Mediterranean Basin. http://www.diam.unige.it/idromet/avi080/altinb.html.
Arnold, D., et al., 2012. Issues in high-resolution atmospheric modeling in complex topography – the HiRCoT workshop. Croat. Meteorol. J. 47, 3–11.
Buzzi, A., Tartaglione, N., Malguzzi, P., 1998. Numerical simulations of the 1994 Piedmont flood: role of orography and moist processes. Mon. Weather Rev. 126, 2369–2383.
Cassola, F., Ferrari, F., Mazzino, A., 2015. Numerical simulations of Mediterranean heavy precipitation events with the WRF model: a verification exercise using different approaches. Atmos. Res. 164-165, 210–225.
Chen, F., Dudhia, J., 2001. Coupling an advanced land-surface/hydrology model with the Penn state/NCAR MM5 modeling system. Part I: model description and implementation. Mon. Weather Rev. 129, 569–585.
Chen, C., Lin, Y., 2005. Orographic effects on a conditionally unstable flow over an idealized three-dimensional mesoscale mountain. Meteorog. Atmos. Phys. 88, 1–21.
Chen, S.H., Sun, W.Y., 2002. A one dimensional time dependent cloud model. J. Meteorol. Soc. Jpn. 80, 99–118.
Chou, M.D., Suarez, M.J., 1994. An Efficient Thermal Infrared Radiation Parameterization for Use in General Circulation Models. (Technical Report) NASA/Goddard Space Flight Center.
Chu, C., Lin, Y., 2000. Effects of orography on the generation and propagation of mesoscale convective systems in a two-dimensional unstable flow. J. Atmos. Sci. 57, 3817–3837.
Clyne, J., Rast, M., 2005. A prototype discovery environment for analyzing and visualizing terascale turbulent fluid flow simulations. In: Erbacher, R.F., Roberts, J.C., Gröhn, M.T., Börner, K. (Eds.), Proc. of SPIE-IS & T Electronic Imaging, pp. 284–294.
Clyne, J., Mininni, P., Norton, A., Rast, M., 2007. Interactive desktop analysis of high resolution simulations: application to turbulent plume dynamics and current sheet formation. New J. Phys. 9, 301–328.
Davolio, S., Buzzi, A., Malguzzi, P., 2006. Orographic influence on deep convection: case study and sensitivity experiments. Meteorol. Z. 15, 215–223.
Davolio, S., Mastrangelo, D., Miglietta, M.M., Drofa, O., Buzzi, A., Malguzzi, P., 2009. High resolution simulations of a flash flood near Venice. Nat. Hazards Earth Syst. Sci. 9, 1671–1678.
De Meiji, A., Vinuesa, J., 2006. Impact of SRTM and Corine Land Cover data on meteorological parameters using WRF. Atmos. Res. 143, 351–370.
Esteve, B.J., 2014. Land Use Influence in WRF Model. A High Resolution Mesoscale Modeling Over Oriental Pyrenees. Master de Meteorologia. Universitat de Barcelona.
Fiori, E., Comellas, A., Molini, L., Rebora, N., Siccardi, F., Gochis, D.J., Tanelli, S., Parodi, A., 2014. Analysis and hindcast simulation of an extreme rainfall event in the Mediterranean area: the Genoa 2011 case. Atmos. Res. 138, 13–29.
Garratt, J., 1993. Sensitivity of climate simulations to land surface and atmospheric boundary-layer treatments – a review. J. Clim. 6, 419–449.
Giuffrida, A., Sansosti, G., 2007. Manuale di Meteorologia. (Gremese editore).
Haltiner, G., Williams, H., 1983a. Numerical Prediction and Dynamic Meteorology. Wiley Sons Ltd.
Haltiner, G.J., Williams, R.T., 1983b. Numerical Prediction and Dynamic Meteorology. Wiley Sons Ltd.
Holton, J.R., 2004. An Introduction to Dynamic Meteorology. Academic Press.
Hoskins, B.J., James, I.,.N., 2014. Fluid Dynamics of the Mid Latitude Atmosphere. Wiley Blackwell.
Janjic, Z.I., 2002. Nonsingular Implementation of the Mellor–Yamada Level 2.5 Scheme in the NCEP Meso Model. (Technical Report 437) NOAA Science Center.
Kain, J.S., 2004. The Kain–Fritsch convective parameterization: an update. J. Appl. Meteorol. 43, 170–181.
Kalnay, L., 2002. Atmospheric Modeling, Data Assimilation and Predictability. Cambridge University Press.
Lackman, G., 2011. Midlatitude Synoptic Meteorology. American Meteorological Society.
Markowski, P., Richardson, Y., 2010. Mesoscale Meteorology in Midlatitudes. Wiley.
Martin, J.E., 2006. Mid-Latitude Atmospheric Dynamics. A First Course. Wiley.
Miglietta, M.M., Buzzi, A., 2001. A numerical study of moist stratified flows over isolated topography. Tellus 53A, 481–499.
Miglietta, M.M., Rotunno, Richard, 2009. Numerical simulations of low-CAPE flows over a mountain ridge. J. Atmos. Sci. 66, 2391–2401.
Mlawer, E.J., Taubman, S.J., Brown, P.D., Iacono, M.J., Clough, S.A., 1997. Radiative transfer for inhomogeneous atmosphere: RRTM, a validated correlated k-model for the long-wave. J. Geophys. Res. 102, 16663–16682.
Morrison, H., Milbrandt, J., 2011. Comparison of two-moment bulk microphysics schemes in idealized supercell thunderstorm simulations. Mon. Weather Rev. 139, 1103–1130.
Pineda, N., Jorba, O., Jorge, J., Baldasano, J.M., 2004. Using NOAA AVHRR and SPOT VGT data to estimate surface parameters: application to a mesoscale meteorological model. Int. J. Remote Sens. 25 (1), 129–143.
Randall, D., 2001. An Introduction to Atmospheric Modelling. Department of Atmospheric Science, Colorado State university, Boulder.
Ray, P., 1986. Mesoscale Meteorology and Forecasting. American Meteorological Society.
Reeves, H.D., Rotunno, R., 2008. Orographic flow response to variations in upstream humidity. J. Atmos. Sci. 66, 3557–3570.
Salby, M.L., 1996. Fundamentals of Atmospheric Physics. Academic Press.
Schicker, I., Seibert, P., 2009. Simulation of the meteorological conditions during a winter smog episode in the Inn Valley. Meteorog. Atmos. Phys. 103, 211–222.
Smith, R., 1979. The influence of mountains on the atmosphere. Adv. Geophys. 21, 87–230.
Stensrud, D.J., 2007. Parametrization Scheme, Cambridge.
Szintai, B., Kaufmann, P., Rotach, M.W., 2010. Simulation of pollutant transport in complex terrain with a numerical weather prediction–particle dispersion model combination. Bound.-Layer Meteorol. 137, 373–396.
Thompson, G., Rasmussen, R.M., Manning, K., 2004. Explicit forecasts of winter precipitation using an improved bulk microphysics scheme. Part I: description and sensitivity analysis. Mon. Weather Rev. 132, 519–542.
Wallace, J.M., Hobbs, P.V., 2006. Atmospheric Science: An Introductory Survey. Academic Press.
Zängl, G., 2007. Interaction between dynamics and cloud microphysics in orographic precipitation enhancement: a high-resolution modeling study of two north alpine heavy-precipitation events. Mon. Weather Rev. 135, 2817–2840.